

Dynamics and Variability of ERK2 Response to EGF in Individual Living Cells

Cellina Cohen-Saidon,^{1,3} Ariel A. Cohen,^{1,3} Alex Sigal,^{1,2} Yuval Liron,¹ and Uri Alon^{1,*}

¹Department of Molecular Cell Biology, Weizmann Institute of Science, Rehovot 76100 Israel

²Present address: Division of Biology, California Institute of Technology, Pasadena, California 91125, USA

³These authors contributed equally to this work

*Correspondence: uri.alon@weizmann.ac.il

DOI 10.1016/j.molcel.2009.11.025

SUMMARY

Signal-transduction cascades are usually studied on cell averages, masking variability between individual cells. To address this, we studied in individual cells the dynamic response of ERK2, a well-characterized MAPK signaling protein, which enters the nucleus upon stimulation. Using fluorescent tagging at the endogenous chromosomal locus, we found that cells show wide basal variation in ERK2 nuclear levels. Upon EGF stimulation, cells show (1) a fold-change response, where peak nuclear accumulation of ERK2 is proportional to basal level in each cell; and (2) exact adaptation in nuclear levels of ERK2, returning to original basal level of each cell. The timing of ERK2 dynamics is more precise between cells than its amplitude. We further found that in some cells ERK2 exhibits a second pulse of nuclear entry, smaller than the first. The present study suggests that this signaling system compensates for natural biological noise: despite large variation in nuclear basal levels, ERK2's fold dynamics is similar between cells.

INTRODUCTION

Human cells respond to signals such as growth factors, cytokines, and hormones by means of signal transduction pathways. These pathways typically culminate in the entry of regulatory proteins into the nucleus, resulting in programs of gene expression. Such signaling systems need to function in the face of large cell-cell variability in protein concentrations, cell size, and other parameters (Barkai and Leibler, 1997; Colman-Lerner et al., 2005; Feinerman et al., 2008; Kaern et al., 2005; McAdams and Arkin, 1997; Sigal et al., 2006b). One may ask the following: How are the dynamics of signaling systems affected by these cell-to-cell variations? Are there specific aspects of the dynamics that are more robust (invariant) to cell-cell variations than other aspects?

To address such questions on cell-cell variability requires studying the response of signaling proteins in individual living cells over time. Standard assays based on averaging cell populations cannot be used, because they mask cell-cell variations,

as well as dynamical features such as all-or-none effects (Ferrell and Machleder, 1998), excitability (Suel et al., 2006, 2007) and oscillations (Cai et al., 2008; Geva-Zatorsky et al., 2006; Hilioti et al., 2008; Lahav et al., 2004; Momiji and Monk, 2008; Nelson et al., 2004). Methods based on flow cytometry can provide snapshots of signaling proteins in individual cells (Feinerman et al., 2008; Sachs et al., 2005); however, they are not able to observe the same cell over time.

Here, we measured the dynamics of nuclear entry of a key signaling protein in individual living cells at high temporal resolution. As a model system, we chose the well-characterized protein ERK2 (extracellular signal-regulated kinase), which belongs to the classical MAPK (mitogen-activated protein kinase) cascade (Boulton et al., 1991; Chang and Karin, 2001; Lewis et al., 1998; Raman et al., 2007; Seger and Krebs, 1995; Shaul and Seger, 2007). ERK2 is a signaling protein that is activated in response to a variety of stimuli, including epidermal growth factor (EGF). Following EGF stimulation, there is a pulse of translocation of ERK into the nucleus (Ando et al., 2004; Chen et al., 1992; Chuderland et al., 2008; Costa et al., 2006; Lenormand et al., 1993; Matsubayashi et al., 2001; Whitehurst et al., 2002). In the nucleus, ERK2 activates transcription factors to trigger cell proliferation or differentiation (Brunet et al., 1999; Meloche and Pouyssegur, 2007). There may be additional avenues of signaling in this system without nuclear translocation of ERK (Dikic et al., 1994; Murphy et al., 2002; Traverse et al., 1994).

To study the dynamics of ERK2, we employed a human cell clone expressing ERK2 tagged with YFP (yellow fluorescent protein) at its endogenous chromosomal locus and under its native regulation. This tagged ERK2 is expressed at lower levels than the untagged alleles in the same cell, and reports faithfully their nuclear entry dynamical profiles, as assayed by immunoblots. We followed the dynamics of ERK2 by quantifying the nuclear intensity of YFP in individual cells using automated time-lapse microscopy. We found that prior to EGF treatment, nuclear levels of ERK2 show wide cell-cell variation. Despite this variability, we found that some aspects of the dynamics upon EGF stimulation are very similar between cells: the relative increase in ERK2 nuclear levels is proportional to basal level of nuclear ERK2 of each cell, suggesting a fold-change response. The timing of this nuclear accumulation is quite precise between cells. Most cells then return to their own prestimulus basal levels, a well-known phenomenon in sensory systems known as exact adaptation. We also find that a subpopulation of cells shows

a second pulse of nuclear entry, a behavior that would be masked by standard cell population methods. The present view of a signaling molecule at the individual cell level suggests that the ERK2 system compensates for the natural biological noise to provide exact adaptation, precise timing, and a fold-change response.

RESULTS

Assay for Following ERK2 Dynamics in Individual Living Cells

For studying the dynamics of ERK2 in individual living cells, we used a clone from the library of annotated reporter cell clones (LARC), based on the H1299 human non-small cell lung cancer cell line (Sigal et al., 2007). The library was built using a tagging approach that introduces YFP as a new exon into the chromosome, using a retrovirus (Figure 1A). This tagging preserves both the native regulation and the chromosomal position of the tagged gene. Study of 20 different endogenously tagged proteins from the LARC library showed that 80% of the YFP-tagged proteins serve as faithful markers for the dynamics of the endogenous proteins (Cohen et al., 2008).

The clone used in this study has YFP introduced as an internal exon into an allele of the ERK2 gene on chromosome 22. YFP is inserted in-frame between exons 1 and 2 of the ERK2 gene. When this gene is transcribed, YFP is spliced into the message producing a full-length fluorescent fusion protein, expressed from its native chromosomal locus, in parallel to untagged ERK2 (Figure 1A).

Immunoblots with anti-ERK2 antibodies show that the tagged ERK2 protein is ~69 kD, which is 27 kD more than the untagged ERK2 in the same cells, corresponding to the molecular weight of YFP (Figures 1B [upper panel] and S1). The tagged ERK2 protein is recognized by monoclonal anti-GFP antibodies (Figure 1B [lower panel]).

We compared the expression of ERK2 from the tagged allele to that of the untagged alleles in the same cells (Figure 1B [upper panel]). We found that the band corresponding to ERK2-YFP is about 4-fold less intense than the untagged ERK2 band, using a monoclonal antibody against the C terminus of ERK2 (Figure 1B [upper panel]) or about 5-fold lower using a polyclonal antibody, which recognizes also ERK1 (Figure S1). One possible reason for this lower expression is that the parental H1299 cells show three copies of chromosome 22 (data not shown), of which only one is expected to be tagged. Thus, ERK2-YFP seems to represent a relatively small fraction (20%–25%) of total cellular ERK2. Note that the present endogenous tagging therefore seems to avoid the overexpression concerns associated with other means of introducing tagged proteins into cells.

The present YFP tag is close to the N terminus of ERK2 (39 amino acids from the terminus). Previous studies have indicated that N-terminal fluorescent fusions (GFP or YFP) to ERK2 do not affect protein localization, phosphorylation, or kinase activity (Vantaggiato et al., 2006; Yung et al., 2001).

To further test the present system, we asked whether ERK2-YFP is capable of nuclear translocation upon EGF stimulation. For this purpose, we monitored the accumulation of ERK2-YFP

in cell nuclei over time. Time-lapse microscopy on these cells showed that the fluorescence intensity of YFP in the nucleus increases after EGF (50 ng/ml) stimulation (Figure 1C; Movie S1), peaks at about 10 min after stimulation, and decays thereafter. Immunoblots on nuclear cell fractions with monoclonal antibody against ERK2 or GFP showed dynamics of ERK2-YFP upon EGF stimulation with similar timing to the movies (Figures 1D and 1E). The dynamic profile of both the tagged and untagged alleles in these immunoblots was also very similar (Figures 1D and 1E). This temporal profile is in line with that reported by previous studies on cell averages or transfected cells (Ando et al., 2004; Chen et al., 1992; Costa et al., 2006; Fujioka et al., 2006; Horgan and Stork, 2003). We also tested the phosphorylation of tagged ERK2 upon stimulation in our cells. Using antibodies against phosphorylated ERK, we found that ERK2-YFP undergoes phosphorylation upon EGF treatment, with similar dynamics for the tagged and untagged ERK2 alleles (data not shown).

Next, we tested whether the nuclear accumulation of ERK2-YFP is dependent on phosphorylation by its upstream kinases, MEK1/2. Pretreatment of the cells with U0126 (10 μ M), a specific MEK inhibitor (Favata et al., 1998), impaired the phosphorylation upon EGF stimulation of both tagged and untagged ERK2, as detected in nuclear fractions (Figure S2A). Movies of cells treated with the MEK inhibitor and stimulated with EGF showed no nuclear accumulation of ERK2-YFP (Figures S2B and S3 [blue line]; Movie S2). Similar abolishment of nuclear entry was observed when treating the cells with a selective inhibitor of the EGF receptor (AG1478) (Levitzi and Gazit, 1995; Ward et al., 1994) (Figure S3 [green line]; Movie S3).

Taken together, these results suggest that the endogenously tagged ERK2-YFP clone can serve as a faithful marker for the nuclear dynamics of native ERK2 protein.

ERK2 Shows Variability in Its Nuclear Basal Levels

To study ERK2-YFP dynamics, we employed automated time-lapse microscopy and image analysis to track ~650 cells individual cells for 5 min before EGF stimulation, and for additional 60 min following EGF stimulation.

The reporter cell library, from which our clone originates, was designed for automated imaging of protein dynamics. These H1299 cells are well suited for imaging due to their nonoverlapping growth and relatively regular shape. Furthermore, to enable automated image analysis, the parental clone of ERK2-YFP cells was tagged with a second, red protein tag (Cohen et al., 2008). This red tag (mCherry) was introduced as an exon into the native locus of a protein with nuclear localization, CBX5 (chromobox 5), which is unrelated to the ERK2 system. This red tag allows automated image analysis to detect the nucleus in each cell. Movies were automatically analyzed for nuclear levels of ERK2-YFP (Cohen et al., 2008; Sigal et al., 2006a).

We measured for each cell the nuclear levels of ERK2-YFP, defined as the median fluorescence pixel intensity in the nucleus, at a temporal resolution of 90 s. We found that prior to EGF stimulation, individual clonal cells show different basal levels of ERK2 nuclear fluorescence intensity (Figures 2A and 2B). The cell-cell variation in basal nuclear level spans about a 4-fold range. The

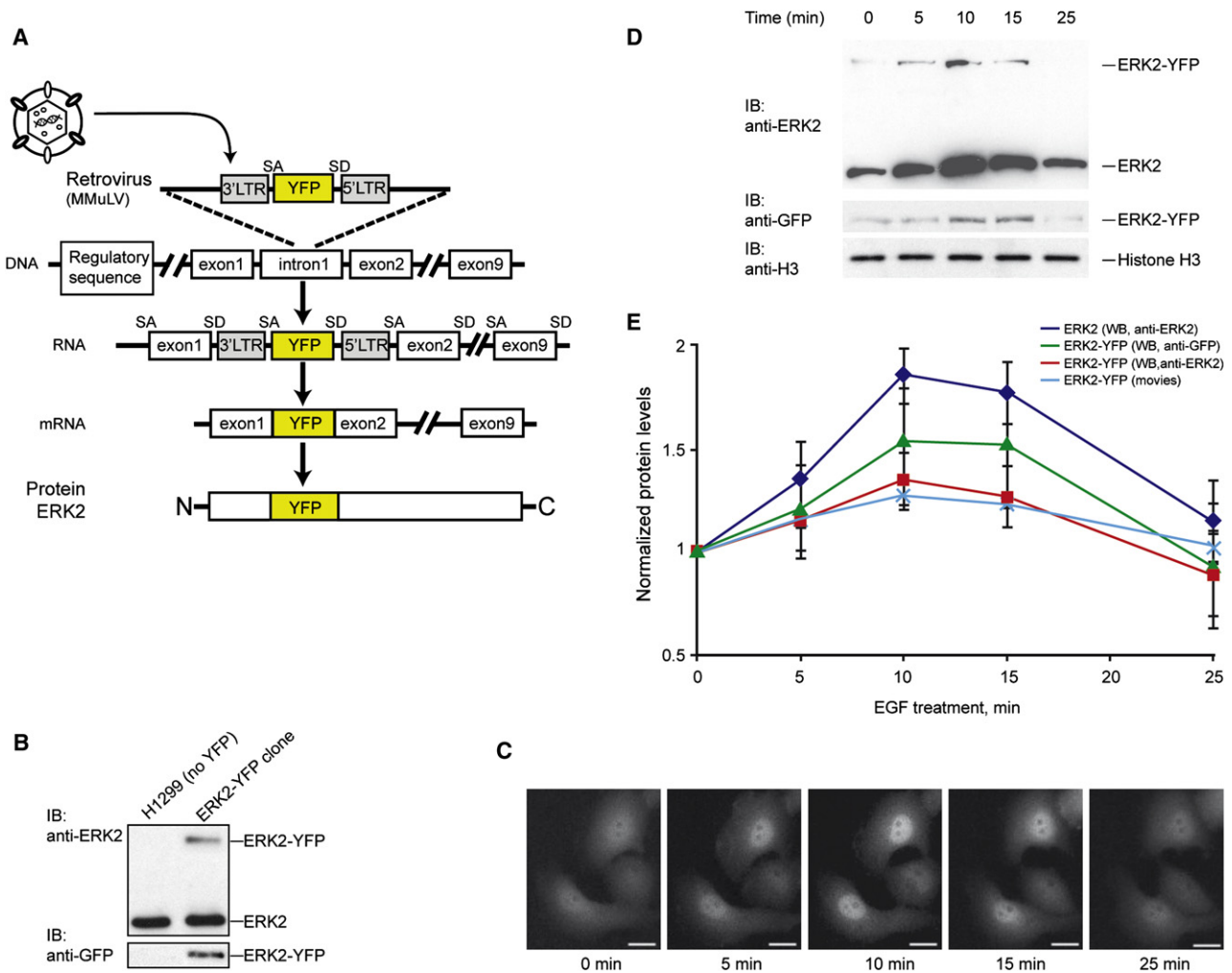


Figure 1. ERK2-YFP Expressed from Its Native Chromosomal Locus Is a Faithful Reporter for Untagged ERK2

(A) Schematic representation of YFP insertion by retroviral infection at intron 1 at the chromosomal locus (chromosome 22) of human ERK2 in a H1299 cell clone (clone C7). Following transcription, YFP is spliced in as an exon and expressed as a fluorescent fused protein.

(B) ERK2-YFP is expressed as a full-length protein in parallel to the native ERK2. Whole-cell lysates from C7 clone and H1299 parental cells were subjected to immunoblotting. ERK2-YFP protein (~69 kD) is detected by monoclonal anti-ERK2 antibody and polyclonal anti-ERK1/2 antibody in parallel to untagged ERK2 protein (~42 kD) in cell clone C7. ERK2-YFP is also recognized by monoclonal anti-GFP antibody.

(C) ERK2-YFP shows translocation into nucleus upon EGF stimulation with a peak at about 10 min. Following serum starvation, cells were transferred into the microscope incubator, visualized by time-lapse microscopy and then stimulated with 50 ng/ml EGF. Bar denotes 10 microns.

(D) ERK2-YFP displays a similar pattern of nuclear accumulation as untagged nuclear ERK2. Nuclear extracts were obtained from C7 cells stimulated with 50 ng/ml EGF for various times (0, 5, 10, 15, 25 min). Detection of ERK2 and ERK2-YFP in nuclear fractions was performed with monoclonal anti-ERK2 antibody. Monoclonal anti-GFP antibody was used for detecting ERK2-YFP. Nuclear histone H3 was used as a control.

(E) ERK2-YFP shows similar dynamics in nuclear accumulation as ERK2. Quantification of the nuclear levels of ERK2 and ERK2-YFP is from both immunoblots and time-lapse microscopy. Red line denotes nuclear protein levels of ERK2-YFP detected by anti-ERK2 antibody, green line denotes its detection by anti-GFP antibodies, blue line denotes nuclear levels of untagged ERK2, and turquoise line denotes ERK2-YFP dynamics from time-lapse movies. Data is mean \pm SE of three independent experiments.

ratio between the median nuclear fluorescence of the 90th percentiles of the cells to the 10th percentile of cells is 3.1 ± 0.6 . This level of variability is comparable with that found in the nuclear levels of other proteins in human cells (Sigal et al., 2006b).

The fact that two proteins are tagged in our cells, one red and the other yellow, allows one to control for global cell effects (size,

protein synthesis capacity) or experimental variations. We found that the nuclear marker, CBX5-mCherry, exhibits a similar range of variability in its nuclear levels as ERK2-YFP (Figure 2C). The levels of the two proteins in the same cell are only mildly correlated ($R = 0.3 \pm 0.1$; $p < 0.001$). This suggests that ERK2 variability has a stochastic component not related to variations in global cell properties (Elowitz et al., 2002).

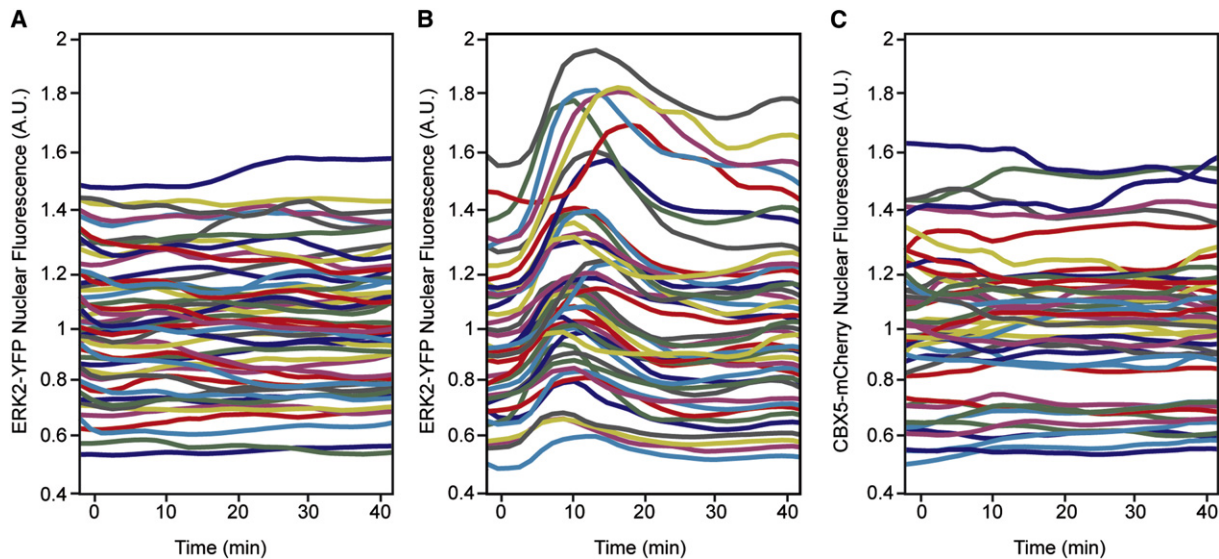


Figure 2. ERK2-YFP Nuclear Intensity Increases and Then Decreases upon EGF Stimulation

Following serum starvation, cells were subjected to time-lapse movies, with a time resolution of 90 s between frames. Nuclear YFP fluorescence intensities of individual cells with tagged ERK2 were measured in response to EGF or mock stimulation added at $t = 0$. (A) ERK2-YFP does not accumulate in the nucleus of mock-treated cells. Lines denote nuclear median pixel fluorescence of ERK2-YFP in individual cells (C7 clone).

(B) ERK2-YFP shows a pulse of accumulation upon EGF treatment. Lines denote nuclear median pixel fluorescence of ERK2-YFP in individual cells (C7 clone). (C) Nuclear levels of CBX5-mCherry protein do not change upon EGF stimulation. Lines denote nuclear median fluorescence of CBX5-mCherry in the same individual cells as in B (clone C7).

Cells Show a Fold-Change Response to EGF, Rather Than an Absolute Response, with Precise Timing

Upon addition of EGF to the medium (50 ng/ml), we find that ERK2-YFP nuclear levels rise, reaching a peak after 13 ± 2.2 min (Figure 2B). The nuclear fluorescence levels then decay. No increase was observed in control experiments with mock stimulation in which medium with no EGF was added to the cells (Figure 2A). Likewise, no increase was observed upon EGF stimulation in the red-tagged nuclear protein in the same cells (Figure 2C).

To quantify the variability in the dynamics, we measured several parameters of the response profile for each cell. We measured the initial nuclear YFP fluorescence level before stimulation (F_i), peak fluorescence (F_{max}), and final fluorescence (F_f), as well as temporal features of the dynamics, the half times for increase (T_{50} up) and decrease (T_{50} down) phases, and the time of peak fluorescence (T_{max}). These parameters are defined Figure 3A, and their values are summarized in Figure 3B. For measuring the cell-cell variability, we used the coefficient of variation (CV), defined by the ratio of the standard deviation to the mean ($CV = SD/mean$), as shown in Figure 3C.

We found that the CV of each of the nuclear fluorescence levels parameters, F_i , F_{max} and F_f , was about 30%, as shown in Figure 3C, blue bars. In contrast, two of the temporal parameters showed smaller cell-cell variability: the timing of the peak intensity, $T_{max} = 13 \pm 2.2$ min, shows a lower variation between cells than fluorescent levels ($CV \sim 0.17$; Figure 3C [red bars]). A low CV was found also for the half-time of the increase in nuclear levels. Larger variations were found in the half-time for nuclear exit. Thus, there is larger cell-cell variability in param-

eters related to protein levels than in parameters for response rise time and peak time.

We also studied the variability in the fold change of the response, defined as the ratio of peak nuclear fluorescence (F_{max}) to basal levels (F_i). Interestingly, we find that cells exhibit a well-defined fold change in nuclear ERK2-YFP levels in response to EGF stimulation. The fold-change response, defined by the ratio F_{max}/F_i , is 1.25 ± 0.11 (mean \pm SD) and has low variability between cells ($CV = 0.09$), as shown in Figure 3C, green bars.

Thus, cells seem to show a rather constant fold increase in ERK2 nuclear levels upon EGF stimulation. Another way to state this is that the increase above the basal level, defined as the difference between the peak nuclear intensity and the initial level ($\Delta F = F_{max} - F_i$) is approximately proportional to the basal level for each cell ($R = 0.59$, $p < 0.001$) (Figure 3D). This means that cells with high initial nuclear ERK2-YFP tend to show a larger absolute increase than cells with low initial ERK2-YFP. This type of response can be termed a “fold-change response,” where the amount of ERK2 entering the nucleus is a constant fraction of the basal level. This is opposed to an “absolute response” in which the amount of ERK2 entering the nucleus is the same between cells, regardless of their basal level.

Nuclear Levels of ERK2-YFP Show Exact Adaptation to the Basal Level of Each Individual Cell

We next asked how exact is the adaptation following the stimulus? For this purpose, we considered the ratio between the final and initial fluorescence levels, F_f/F_i . We find that in about 80% of the cells, the nuclear levels of ERK2-YFP return to within 10% of

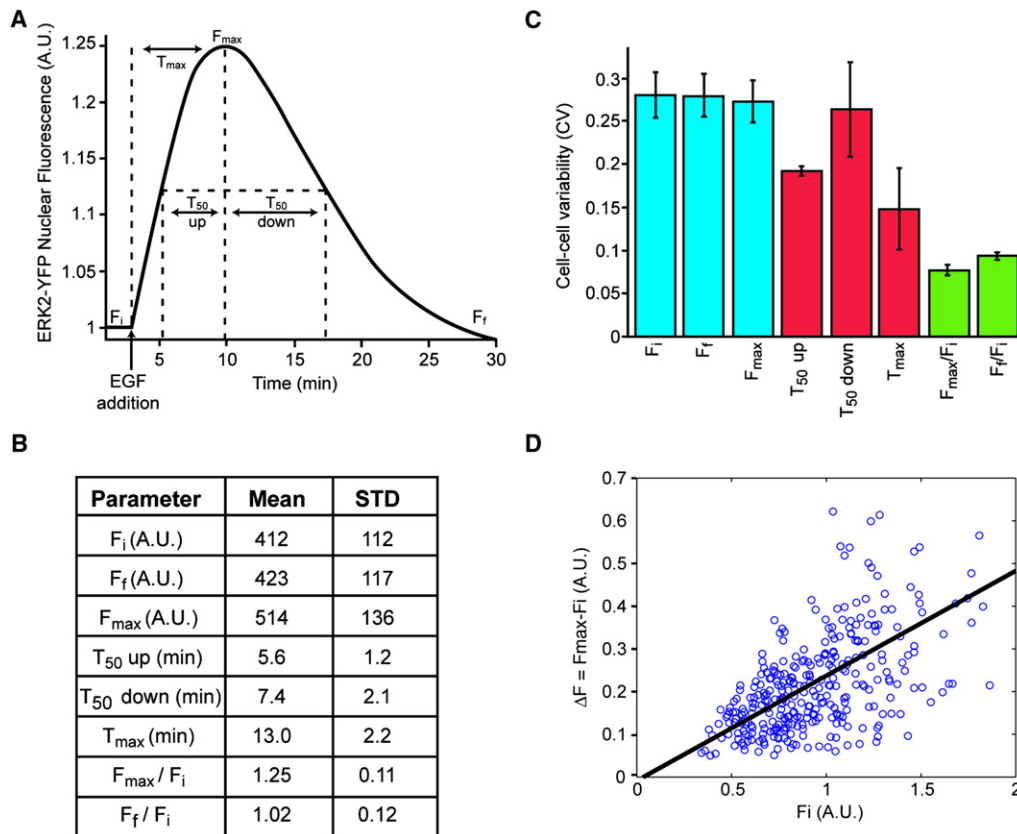


Figure 3. Parameters of Nuclear Protein Level Are More Variable than Most Timing Parameters

(A) Definition of parameters in the nuclear accumulation pattern of YFP-tagged ERK2 in response to EGF stimulation. F_i denotes the initial fluorescence at $t = 0$, F_f is the fluorescence at $t = 30$ min after EGF addition, and F_{max} denotes the maximum fluorescence; $T_{50\text{ up}}$ denotes the time to reach 50% of maximal fluorescence during nuclear fluorescence buildup (minutes), $T_{50\text{ down}}$ denotes the time to reach 50% of maximal fluorescence decrease (minutes), and T_{max} denotes the times to reach the maximal fluorescence. All fluorescence measurements are nuclear median YFP pixel fluorescence, normalized to mCherry in the same pixels.

(B) Values of parameters characterizing the dynamics of ERK2. Values were obtained from time-lapse movies of EGF-stimulated cells (mean and standard deviation between cells), and represent median nuclear YFP/mCherry fluorescence.

(C) Cell-cell variability measured as the CV (ratio of standard deviation to mean) of different aspects of ERK2 response. Blue bars represent measurements of fluorescence level parameters, red bars represent measurements of timing parameters, and green bars represent the ratios of fluorescence levels. Error bars are standard errors.

(D) Increase in nuclear fluorescence levels upon EGF stimulation is correlated with initial fluorescence F_i in each cell. Nuclear levels of YFP were normalized to the mCherry. Each circle is a measurement obtained from an individual cell. Black line represents the best linear fit ($R = 0.59$, $p < 0.0001$).

the original, prestimulus basal level. This occurs on a timescale of 25 min after EGF stimulation (Figure 2B). The average adaptation ratio is close to one: $F_f/F_i = 1.02 \pm 0.12$ (mean \pm SD) with a CV = 0.12 (Figure 3C [green bars]). Thus, ERK2 shows precise adaptation in nuclear levels, returning to the original basal level in the majority of cells.

Some Cells Show a Second Peak of ERK2 Nuclear Entry

Data analysis and manual inspection of the time-lapse movies revealed that a fraction of the cells displayed a second peak of ERK2 nuclear entry (Figure 4A, Movie S4). To quantitate this, we operationally defined a second peak as a sharp rise of at least 5% in nuclear levels after the end of the first nuclear accumulation, i.e., after 25 min (Figure 4B). The fraction of the cells that showed a second peak varied between experiments, within the range 0.4 ± 0.2 (mean \pm SD) across four movies.

Despite attention to experimental protocol, we could not find what conditions corresponded to the variation in the fraction of cells that display the second peak. The timing of the second peak is quite uniform between cells, about 40 ± 9 min (mean \pm SD) after EGF stimulation. Its fold change was lower than the first peak, averaging 1.11 ± 0.03 compared to 1.25 ± 0.11 (Figure 4C).

Such a second peak is likely to be masked in immunoblots and other methods that assay cell averages, because of its low amplitude and appearance in only a fraction of the cells.

DISCUSSION

This study provides a view of a signaling protein, ERK2, responding to its stimulus, EGF, in individual living cells. Nuclear localization of ERK2 was followed at high temporal resolution and

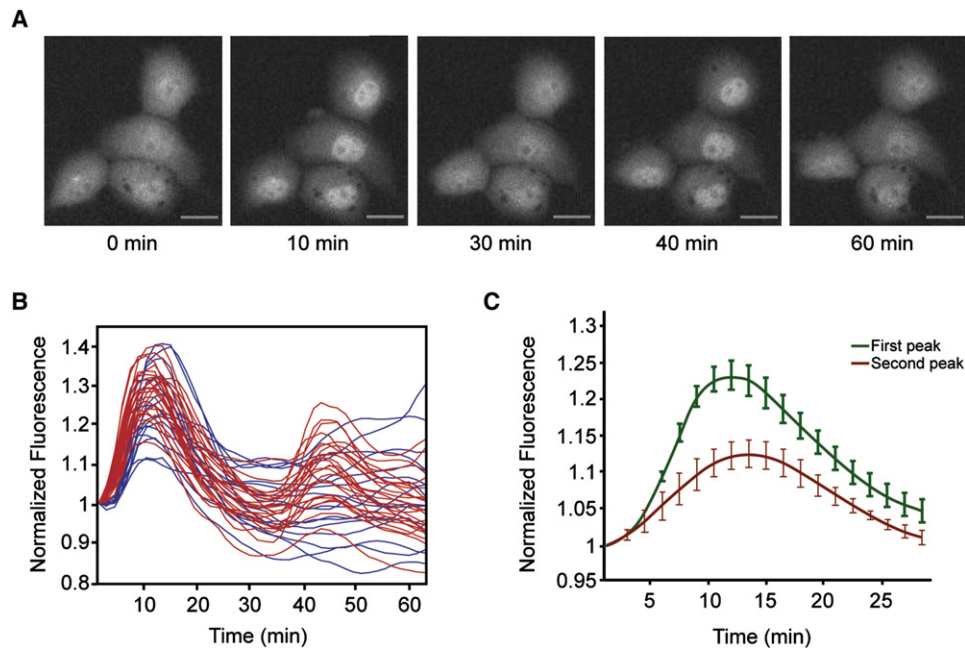


Figure 4. Some Cells Show a Second Peak after EGF Stimulation

(A) Some cells show a second peak of response to EGF. Filmstrip showing two peaks of nuclear accumulation of ERK2-YFP in response to EGF stimulation. Following serum starvation, cells were transferred into the microscope incubator, visualized by time-lapse microscopy, and then stimulated with 50 ng/ml EGF. Bars are 10 microns.

(B) Nuclear fluorescence intensities of individual cells with YFP tagged ERK2, in response to EGF, normalized to the initial time point. Lines denote median nuclear YFP fluorescence in individual cells. Blue line represents cells with a single peak cells, and red line represents cells with two peaks, defined as cells showing a sharp increase of more than 5% in nuclear fluorescence levels after 25 min.

(C) The second peak of nuclear accumulation of ERK2-YFP, normalized to initial levels, shows similar timing and lower amplitude. The second peak of ERK2-YFP response was shifted in time to be superimposed on the first peak. Lines represent averages over experiments and bars are standard errors. Green line denotes the first peak; red line denotes the second peak.

accuracy using an endogenously tagged ERK2-YFP cell line clone. This approach preserves native regulation and avoids overexpression concerns, and seems to faithfully report for the endogenous protein dynamics. We find that basal nuclear levels of ERK2-YFP show about 4-fold cell-cell variations. Despite this variation, the dynamical profiles normalized to the basal level are similar between cells. We find that the amount of ERK2 entering the nucleus upon EGF stimulation is proportional to the basal level of nuclear ERK2-YFP in each cell, suggesting a fold-change response mechanism. This means that the more ERK2 is initially in the nucleus, the more ERK2 accumulates in the nucleus following EGF stimulation.

The present data seems to rule out an “absolute response” mechanism for ERK2 nuclear accumulation, in which the response is independent of basal levels. The question of fold change versus absolute change is an interesting one, which has been rarely studied in molecular systems. The fold-change response suggested by the present data raises the question whether downstream targets of ERK2 respond to ERK2 fold or absolute changes. This can be studied in principle by extending the present approach to tag both ERK2 and a downstream target in the same cell with different fluorescent colors (Sigal et al., 2006b).

In an accompanying paper, Goentoro and Kirschner present experimental evidence on the Wnt pathway indicating that fold

changes rather than absolute levels of β -catenin regulate both gene expression and embryo shape during frog development (Goentoro and Kirschner, 2009). In contrast, an absolute-response mechanism seems to occur in some bacterial two-component systems (Goulian, 2004; Shinar et al., 2007). For example, in the EnvZ/OmpR two-component system of *E. coli*, the amount of phosphorylated response regulator OmpR-P appears to be independent of the total level of OmpR in the cell. It would be fascinating to study which molecular systems detect fold changes in input and which do not.

We further find that cells exhibit exact adaptation in their nuclear levels of ERK2-YFP following EGF stimulation. Such exact adaptation, in which nuclear levels return to the baseline of each individual cell, is a feature shared with other sensory systems. The fact that cells differ widely in their basal levels, but can still precisely adapt, suggests that exact adaptation in this system is robust to variations in protein levels and conditions between cells. Mechanisms for such robust exact adaptation have been studied in the context of bacterial chemotaxis (Alon, 2006; Alon et al., 1999; Barkai and Leibler, 1997) and other systems (Levchenko and Iglesias, 2002; Tyson et al., 2003), and have been related to the engineering principle of integral feedback (El-Samad et al., 2002; Muzzey et al., 2009; Yi et al., 2000) or to incoherent feed-forward loops (Ma et al., 2009). It is

intriguing to consider whether analogous mechanisms might be involved in the adaptation in this system.

The present imaging of individual living cells allowed observation of two nuclear peaks of ERK2 following stimulation in a fraction of the cells. Previous studies using immunoblots reported a second increase in phosphorylation levels of ERK2 in 60 min following upon EGF stimulation of hepatocytes (Ebner et al., 2007), and more recently, oscillatory behavior of ERK activity was reported upon activation (Nakayama et al., 2008; Shin et al., 2009). Other studies find ERK oscillations that follow temporal changes in development (Maeda et al., 2004), and in memory formation (Eckel-Mahan et al., 2008). Oscillations in ERK activity have been also predicted based on theoretical analysis (Kholodenko, 2000).

The second peak of nuclear ERK2 might represent a second pulse of signaling in the MAPK cascade. One possible source of delayed signaling is Ras residing in organelles other than the cell membrane (Bivona et al., 2003; Perez de Castro et al., 2004; Tian et al., 2007). Activation of Ras at the plasma membrane by growth factor is rapid and transient while Ras activation in Golgi is delayed and sustained (Chiu et al., 2002; Perez de Castro et al., 2004; Rocks et al., 2006). Other possible mechanisms include oscillatory mechanisms involving negative feedback (Alon, 2006; Geva-Zatorsky et al., 2006; Kholodenko, 2000; Novak and Tyson, 2008; Romond et al., 1999; Sasagawa et al., 2005).

As molecular components become better characterized, it is becoming possible to build quantitative models of how proteins work together to transduce signals (Asthagiri and Lauffenburger, 2001; Birtwistle et al., 2007; Fujjoka et al., 2006). Constraining such models requires physiological data in individual cells (van Oudenaarden and Muzzey, 2009). One such important constraint is knowing which properties of the response vary from cell to cell—and which are robust between cells (Spencer et al., 2009). We find that concentration parameters (basal levels, peak heights) of the ERK2 response seem to vary much more from cell to cell than some of the timing parameters (half-times for increase, peak time). The relative robustness of timing parameters as compared to amplitudes may be a common feature of biological dynamics. It was observed, for example, in p53 oscillations (Geva-Zatorsky et al., 2006; Lahav et al., 2004), and circadian oscillations (Mihalcescu et al., 2004).

The present observations raise the question of what mechanisms might allow downstream genes to respond to fold rather than to absolute levels of phosphorylated ERK2? One possible answer to this question is presented in an accompanying paper by Goentoro and colleagues (Goentoro et al., 2009), which suggests a theoretical mechanism for detection of fold changes based on the incoherent feedforward loop network motif (Alon, 2007).

In summary, studying ERK2 dynamics in individual cells shows that ERK2 displays precision of timing, adaptation, and fold-change response despite large variation in ERK2 nuclear basal levels. In a fraction of cells, two peaks of ERK2 nuclear entry occur following stimulation. The present approach can be extended to study other signaling systems in individual cells, and to determine which aspects of their dynamics are most robust to cell-cell variations.

EXPERIMENTAL PROCEDURES

YFP CD Tagging of Endogenous Proteins

The library of exon-tagged proteins in the H1299 non-small cell carcinoma cell line was previously described (Sigal et al., 2007). The clone used in this research is named C7 (accession number ENSG00000100030).

Cell Culture

Cells (ERK2-YFP clone C7) were maintained in complete RPMI medium (GIBCO) supplied with 10% FCS (GIBCO) and 1% Pen/Strep (Biological Industries, Israel).

Live Cell Microscopy

For movies, cells were seeded at a density of 15,000 cells per well on 12-well coverslip optical plate (MatTek) coated with fibronectin (Sigma) and grown for 24 hr. Following serum starvation for 12 hr, the medium was replaced with 2 ml transparent medium (Biological Industries, Israel) and cells were transferred into the microscope incubator. For stimulation under the microscope, half of the transparent medium (1 ml) was replaced by EGF diluted in transparent medium (1 ml) or only transparent medium (mock). The same procedure was used for inhibitor studies with U0126 (Sigma) or AG1478 (Calbiochem). For a full description, see the [Supplemental Experimental Procedures](#).

Immunoblotting

Western blots were performed on whole cell lysates or nuclear extracts from C7 clone, using the following antibodies: mouse anti-ERK2 (sc-1643, Santa Cruz), rabbit anti-ERK1/2 (9102, Cell Signaling Technologies), mouse anti-phosphorylated ERK1/2 (9106, Cell Signaling Technologies), mouse anti-GFP (Roche), and rabbit anti-Histone H3 (sc-10809, Santa Cruz). Secondary antibodies were from Jackson Laboratories, Maine. For full description, see the [Supplemental Experimental Procedures](#).

Nuclear Fractionation

Nuclei were extracted using a nondetergent method and mechanical disruption using NucBuster Protein Extraction Kit (Novagen, Germany) together with a cocktail of phosphatase inhibitors (Sigma). For full description, see the [Supplemental Experimental Procedures](#).

Time-Lapse Microscopy

Time-lapse movies were obtained at 20× magnification with a time resolution of 90 s. Each time point included three images: phase contrast, red fluorescence, and yellow fluorescence. For full description, see the [Supplemental Experimental Procedures](#).

Image Analysis of Time-Lapse Movies

We used a custom written image analysis tool developed using the Matlab image processing toolbox environment (Mathworks, Natick, MA), as previously described (Sigal et al., 2006a). Nuclei were segmented based on the cherry-tagged protein CBX5 using a combination of thresholding and watershed algorithms. For a fuller description, see the [Supplemental Experimental Procedures](#).

Statistical Data

Cell-cell differences of all parameters describing the dynamical shaped response were quantified using the coefficient of variation (CV) defined as the ratio of standard deviation over the mean. For a full description, see the [Supplemental Experimental Procedures](#).

SUPPLEMENTAL DATA

Supplemental Data include three figures, four movies, Supplemental Experimental Procedures, and Supplemental References and can be found online at [http://www.cell.com/molecular-cell/supplemental/S1097-2765\(09\)00866-1](http://www.cell.com/molecular-cell/supplemental/S1097-2765(09)00866-1).

ACKNOWLEDGMENTS

We thank the Kahn Family Foundation for support. C.C.-S. thanks the Weizmann Institute postdoctoral fellowship. We thank Rony Seger, Shalev Itzkovitz, Laura Sontag-Kleiman, Anat Bren, Naama Geva-Zatorsky, Erez Dekel, Elad Noor, Daniel Koster, Ron Milo, Alon Zaslaver, and members of Alon lab for comments and helpful discussions. We thank Pierre Choukroun for assistance with the computer cluster. Special thanks to Yair Goldberg, Omer Reingold, Nir Shavit, and Shmuel Saïdon for useful comments and insights in the statistical interpretation of the data.

Received: April 6, 2009

Revised: June 2, 2009

Accepted: August 8, 2009

Published: December 10, 2009

REFERENCES

- Alon, U. (2006). *An Introduction to Systems Biology: Design Principles of Biological Circuits* (Boca Raton, FL: Chapman & Hall/CRC).
- Alon, U. (2007). Network motifs: theory and experimental approaches. *Nat. Rev. Genet.* 8, 450–461.
- Alon, U., Surette, M.G., Barkai, N., and Leibler, S. (1999). Robustness in bacterial chemotaxis. *Nature* 397, 168–171.
- Ando, R., Mizuno, H., and Miyawaki, A. (2004). Regulated fast nucleocytoplasmic shuttling observed by reversible protein highlighting. *Science* 306, 1370–1373.
- Asthagiri, A.R., and Lauffenburger, D.A. (2001). A computational study of feedback effects on signal dynamics in a mitogen-activated protein kinase (MAPK) pathway model. *Biotechnol. Prog.* 17, 227–239.
- Barkai, N., and Leibler, S. (1997). Robustness in simple biochemical networks. *Nature* 387, 913–917.
- Birtwistle, M.R., Hatakeyama, M., Yumoto, N., Ogunnaïke, B.A., Hoek, J.B., and Kholodenko, B.N. (2007). Ligand-dependent responses of the ErbB signaling network: experimental and modeling analyses. *Mol. Syst. Biol.* 3, 144.
- Bivona, T.G., Perez De Castro, I., Ahearn, I.M., Grana, T.M., Chiu, V.K., Locker, P.J., Cullen, P.J., Pellicer, A., Cox, A.D., and Philips, M.R. (2003). Phospholipase Cgamma activates Ras on the Golgi apparatus by means of RasGRP1. *Nature* 424, 694–698.
- Boulton, T.G., Nye, S.H., Robbins, D.J., Ip, N.Y., Radziejewska, E., Morgenbesser, S.D., DePinho, R.A., Panayotatos, N., Cobb, M.H., and Yancopoulos, G.D. (1991). ERKs: a family of protein-serine/threonine kinases that are activated and tyrosine phosphorylated in response to insulin and NGF. *Cell* 65, 663–675.
- Brunet, A., Roux, D., Lenormand, P., Dowd, S., Keyse, S., and Pouyssegur, J. (1999). Nuclear translocation of p42/p44 mitogen-activated protein kinase is required for growth factor-induced gene expression and cell cycle entry. *EMBO J.* 18, 664–674.
- Cai, L., Dalal, C.K., and Elowitz, M.B. (2008). Frequency-modulated nuclear localization bursts coordinate gene regulation. *Nature* 455, 485–490.
- Chang, L., and Karin, M. (2001). Mammalian MAP kinase signalling cascades. *Nature* 410, 37–40.
- Chen, R.H., Sarnacki, C., and Blenis, J. (1992). Nuclear localization and regulation of erk- and rsk-encoded protein kinases. *Mol. Cell. Biol.* 12, 915–927.
- Chiu, V.K., Bivona, T., Hach, A., Sajous, J.B., Silletti, J., Wiener, H., Johnson, R.L., 2nd, Cox, A.D., and Philips, M.R. (2002). Ras signalling on the endoplasmic reticulum and the Golgi. *Nat. Cell Biol.* 4, 343–350.
- Chuderland, D., Konson, A., and Seger, R. (2008). Identification and characterization of a general nuclear translocation signal in signaling proteins. *Mol. Cell* 31, 850–861.
- Cohen, A.A., Geva-Zatorsky, N., Eden, E., Frenkel-Morgenstern, M., Issaeva, I., Sigal, A., Milo, R., Cohen-Saidon, C., Liron, Y., Kam, Z., et al. (2008). Dynamic proteomics of individual cancer cells in response to a drug. *Science* 322, 1511–1516.
- Colman-Lerner, A., Gordon, A., Serra, E., Chin, T., Resnekov, O., Endy, D., Pesce, C.G., and Brent, R. (2005). Regulated cell-to-cell variation in a cell-fate decision system. *Nature* 437, 699–706.
- Costa, M., Marchi, M., Cardarelli, F., Roy, A., Beltram, F., Maffei, L., and Ratto, G.M. (2006). Dynamic regulation of ERK2 nuclear translocation and mobility in living cells. *J. Cell Sci.* 119, 4952–4963.
- Dikic, I., Schlessinger, J., and Lax, I. (1994). PC12 cells overexpressing the insulin receptor undergo insulin-dependent neuronal differentiation. *Curr. Biol.* 4, 702–708.
- Ebner, H.L., Blatzer, M., Nawaz, M., and Krumschnabel, G. (2007). Activation and nuclear translocation of ERK in response to ligand-dependent and -independent stimuli in liver and gill cells from rainbow trout. *J. Exp. Biol.* 210, 1036–1045.
- Eckel-Mahan, K.L., Phan, T., Han, S., Wang, H., Chan, G.C., Scheiner, Z.S., and Storm, D.R. (2008). Circadian oscillation of hippocampal MAPK activity and cAmp: implications for memory persistence. *Nat. Neurosci.* 11, 1074–1082.
- El-Samad, H., Goff, J.P., and Khammash, M. (2002). Calcium homeostasis and parturient hypocalcemia: an integral feedback perspective. *J. Theor. Biol.* 214, 17–29.
- Elowitz, M.B., Levine, A.J., Siggia, E.D., and Swain, P.S. (2002). Stochastic gene expression in a single cell. *Science* 297, 1183–1186.
- Favata, M.F., Horiuchi, K.Y., Manos, E.J., Daulerio, A.J., Stradley, D.A., Feeser, W.S., Van Dyk, D.E., Pitts, W.J., Earl, R.A., Hobbs, F., et al. (1998). Identification of a novel inhibitor of mitogen-activated protein kinase. *J. Biol. Chem.* 273, 18623–18632.
- Feinerman, O., Veiga, J., Dorfman, J.R., Germain, R.N., and Altan-Bonnet, G. (2008). Variability and robustness in T cell activation from regulated heterogeneity in protein levels. *Science* 321, 1081–1084.
- Ferrell, J.E., Jr., and Machleder, E.M. (1998). The biochemical basis of an all-or-none cell fate switch in *Xenopus* oocytes. *Science* 280, 895–898.
- Fujioka, A., Terai, K., Itoh, R.E., Aoki, K., Nakamura, T., Kuroda, S., Nishida, E., and Matsuda, M. (2006). Dynamics of the Ras/ERK MAPK cascade as monitored by fluorescent probes. *J. Biol. Chem.* 281, 8917–8926.
- Geva-Zatorsky, N., Rosenfeld, N., Itzkovitz, S., Milo, R., Sigal, A., Dekel, E., Yarnitzky, T., Liron, Y., Polak, P., Lahav, G., and Alon, U. (2006). Oscillations and variability in the p53 system. *Mol. Syst. Biol.* 2, 2006.0033.
- Goentoro, L., and Kirschner, M.W. (2009). Evidence that fold change, and not absolute level, of β -catenin dictates Wnt signaling. *Mol. Cell* 36, this issue, 872–884.
- Goentoro, L., Shoval, O., Kirschner, M.W., and Alon, U. (2009). The incoherent feedforward loop can provide fold response in gene regulation. *Mol. Cell* 36, this issue, 872–884.
- Goulian, M. (2004). Robust control in bacterial regulatory circuits. *Curr. Opin. Microbiol.* 7, 198–202.
- Hilioti, Z., Sabbagh, W., Jr., Paliwal, S., Bergmann, A., Goncalves, M.D., Bardwell, L., and Levchenko, A. (2008). Oscillatory phosphorylation of yeast Fus3 MAP kinase controls periodic gene expression and morphogenesis. *Curr. Biol.* 18, 1700–1706.
- Horgan, A.M., and Stork, P.J. (2003). Examining the mechanism of Erk nuclear translocation using green fluorescent protein. *Exp. Cell Res.* 285, 208–220.
- Kaern, M., Elston, T.C., Blake, W.J., and Collins, J.J. (2005). Stochasticity in gene expression: from theories to phenotypes. *Nat. Rev. Genet.* 6, 451–464.
- Kholodenko, B.N. (2000). Negative feedback and ultrasensitivity can bring about oscillations in the mitogen-activated protein kinase cascades. *Eur. J. Biochem.* 267, 1583–1588.
- Lahav, G., Rosenfeld, N., Sigal, A., Geva-Zatorsky, N., Levine, A.J., Elowitz, M.B., and Alon, U. (2004). Dynamics of the p53-Mdm2 feedback loop in individual cells. *Nat. Genet.* 36, 147–150.

- Lenormand, P., Sartet, C., Pages, G., L'Allemain, G., Brunet, A., and Pouyssegur, J. (1993). Growth factors induce nuclear translocation of MAP kinases (p42mapk and p44mapk) but not of their activator MAP kinase kinase (p45mapkk) in fibroblasts. *J. Cell Biol.* *122*, 1079–1088.
- Levchenko, A., and Iglesias, P.A. (2002). Models of eukaryotic gradient sensing: application to chemotaxis of amoebae and neutrophils. *Biophys. J.* *82*, 50–63.
- Levitzki, A., and Gazit, A. (1995). Tyrosine kinase inhibition: an approach to drug development. *Science* *267*, 1782–1788.
- Lewis, T.S., Shapiro, P.S., and Ahn, N.G. (1998). Signal transduction through MAP kinase cascades. *Adv. Cancer Res.* *74*, 49–139.
- Ma, W., Trusina, A., El-Samad, H., Lim, W.A., and Tang, C. (2009). Defining network topologies that can achieve biochemical adaptation. *Cell* *138*, 760–773.
- Maeda, M., Lu, S., Shauly, G., Miyazaki, Y., Kuwayama, H., Tanaka, Y., Kuspa, A., and Loomis, W.F. (2004). Periodic signaling controlled by an oscillatory circuit that includes protein kinases ERK2 and PKA. *Science* *304*, 875–878.
- Matsubayashi, Y., Fukuda, M., and Nishida, E. (2001). Evidence for existence of a nuclear pore complex-mediated, cytosol-independent pathway of nuclear translocation of ERK MAP kinase in permeabilized cells. *J. Biol. Chem.* *276*, 41755–41760.
- McAdams, H.H., and Arkin, A. (1997). Stochastic mechanisms in gene expression. *Proc. Natl. Acad. Sci. USA* *94*, 814–819.
- Meloche, S., and Pouyssegur, J. (2007). The ERK1/2 mitogen-activated protein kinase pathway as a master regulator of the G1- to S-phase transition. *Oncogene* *26*, 3227–3239.
- Mihalcescu, I., Hsing, W., and Leibler, S. (2004). Resilient circadian oscillator revealed in individual cyanobacteria. *Nature* *430*, 81–85.
- Momiji, H., and Monk, N.A. (2008). Dissecting the dynamics of the Hes1 genetic oscillator. *J. Theor. Biol.* *254*, 784–798.
- Murphy, L.O., Smith, S., Chen, R.H., Fingar, D.C., and Blenis, J. (2002). Molecular interpretation of ERK signal duration by immediate early gene products. *Nat. Cell Biol.* *4*, 556–564.
- Muzzey, D., Gomez-Urbe, C.A., Mettetal, J.T., and van Oudenaarden, A. (2009). A systems-level analysis of perfect adaptation in yeast osmoregulation. *Cell* *138*, 160–171.
- Nakayama, K., Satoh, T., Igari, A., Kageyama, R., and Nishida, E. (2008). FGF induces oscillations of Hes1 expression and Ras/ERK activation. *Curr. Biol.* *18*, R332–R334.
- Nelson, D.E., See, V., Nelson, G., and White, M.R. (2004). Oscillations in transcription factor dynamics: a new way to control gene expression. *Biochem. Soc. Trans.* *32*, 1090–1092.
- Novak, B., and Tyson, J.J. (2008). Design principles of biochemical oscillators. *Nat. Rev. Mol. Cell Biol.* *9*, 981–991.
- Perez de Castro, I., Bivona, T.G., Philips, M.R., and Pellicer, A. (2004). Ras activation in Jurkat T cells following low-grade stimulation of the T-cell receptor is specific to N-Ras and occurs only on the Golgi apparatus. *Mol. Cell. Biol.* *24*, 3485–3496.
- Raman, M., Chen, W., and Cobb, M.H. (2007). Differential regulation and properties of MAPKs. *Oncogene* *26*, 3100–3112.
- Rocks, O., Peyker, A., and Bastiaens, P.I. (2006). Spatio-temporal segregation of Ras signals: one ship, three anchors, many harbors. *Curr. Opin. Cell Biol.* *18*, 351–357.
- Romond, P.C., Rustici, M., Gonze, D., and Goldbeter, A. (1999). Alternating oscillations and chaos in a model of two coupled biochemical oscillators driving successive phases of the cell cycle. *Ann. N Y Acad. Sci.* *879*, 180–193.
- Sachs, K., Perez, O., Pe'er, D., Lauffenburger, D.A., and Nolan, G.P. (2005). Causal protein-signaling networks derived from multiparameter single-cell data. *Science* *308*, 523–529.
- Sasagawa, S., Ozaki, Y., Fujita, K., and Kuroda, S. (2005). Prediction and validation of the distinct dynamics of transient and sustained ERK activation. *Nat. Cell Biol.* *7*, 365–373.
- Seeger, R., and Krebs, E.G. (1995). The MAPK signaling cascade. *FASEB J.* *9*, 726–735.
- Shaul, Y.D., and Seger, R. (2007). The MEK/ERK cascade: from signaling specificity to diverse functions. *Biochim. Biophys. Acta* *1773*, 1213–1226.
- Shin, S.Y., Rath, O., Choo, S.M., Fee, F., McFerran, B., Kolch, W., and Cho, K.H. (2009). Positive- and negative-feedback regulations coordinate the dynamic behavior of the Ras-Raf-MEK-ERK signal transduction pathway. *J. Cell Sci.* *122*, 425–435.
- Shinar, G., Milo, R., Martinez, M.R., and Alon, U. (2007). Input output robustness in simple bacterial signaling systems. *Proc. Natl. Acad. Sci. USA* *104*, 19931–19935.
- Sigal, A., Danon, T., Cohen, A., Milo, R., Geva-Zatorsky, N., Lustig, G., Liron, Y., Alon, U., and Perzov, N. (2007). Generation of a fluorescently labeled endogenous protein library in living human cells. *Nat. Protoc.* *2*, 1515–1527.
- Sigal, A., Milo, R., Cohen, A., Geva-Zatorsky, N., Klein, Y., Alaluf, I., Swerdlin, N., Perzov, N., Danon, T., Liron, Y., et al. (2006a). Dynamic proteomics in individual human cells uncovers widespread cell-cycle dependence of nuclear proteins. *Nat. Methods* *3*, 525–531.
- Sigal, A., Milo, R., Cohen, A., Geva-Zatorsky, N., Klein, Y., Liron, Y., Rosenfeld, N., Danon, T., Perzov, N., and Alon, U. (2006b). Variability and memory of protein levels in human cells. *Nature* *444*, 643–646.
- Spencer, S.L., Gaudet, S., Albeck, J.G., Burke, J.M., and Sorger, P.K. (2009). Non-genetic origins of cell-to-cell variability in TRAIL-induced apoptosis. *Nature* *459*, 428–432.
- Suel, G.M., Garcia-Ojalvo, J., Liberman, L.M., and Elowitz, M.B. (2006). An excitable gene regulatory circuit induces transient cellular differentiation. *Nature* *440*, 545–550.
- Suel, G.M., Kulkarni, R.P., Dworkin, J., Garcia-Ojalvo, J., and Elowitz, M.B. (2007). Tunability and noise dependence in differentiation dynamics. *Science* *315*, 1716–1719.
- Tian, T., Harding, A., Inder, K., Plowman, S., Parton, R.G., and Hancock, J.F. (2007). Plasma membrane nanoswitches generate high-fidelity Ras signal transduction. *Nat. Cell Biol.* *9*, 905–914.
- Traverse, S., Seedorf, K., Paterson, H., Marshall, C.J., Cohen, P., and Ullrich, A. (1994). EGF triggers neuronal differentiation of PC12 cells that overexpress the EGF receptor. *Curr. Biol.* *4*, 694–701.
- Tyson, J.J., Chen, K.C., and Novak, B. (2003). Sniffers, buzzers, toggles and blinkers: dynamics of regulatory and signaling pathways in the cell. *Curr. Opin. Cell Biol.* *15*, 221–231.
- van Oudenaarden, A., and Muzzey, D. (2009). Single-Cell Microscopy, Systems Biology, and Modeling Approaches in Cell Biology. *Annu. Rev. Cell Dev. Biol.* *25*, 301.
- Vantaggiato, C., Formentini, I., Bondanza, A., Bonini, C., Naldini, L., and Brambilla, R. (2006). ERK1 and ERK2 mitogen-activated protein kinases affect Ras-dependent cell signaling differentially. *J. Biol.* *5*, 14.
- Ward, W.H., Cook, P.N., Slater, A.M., Davies, D.H., Holdgate, G.A., and Green, L.R. (1994). Epidermal growth factor receptor tyrosine kinase. Investigation of catalytic mechanism, structure-based searching and discovery of a potent inhibitor. *Biochem Pharmacol* *48*, 659–666.
- Whitehurst, A.W., Wilsbacher, J.L., You, Y., Luby-Phelps, K., Moore, M.S., and Cobb, M.H. (2002). ERK2 enters the nucleus by a carrier-independent mechanism. *Proc. Natl. Acad. Sci. USA* *99*, 7496–7501.
- Yi, T.M., Huang, Y., Simon, M.I., and Doyle, J. (2000). Robust perfect adaptation in bacterial chemotaxis through integral feedback control. *Proc. Natl. Acad. Sci. USA* *97*, 4649–4653.
- Yung, Y., Yao, Z., Aebersold, D.M., Hanoch, T., and Seger, R. (2001). Altered regulation of ERK1b by MEK1 and PTP-SL and modified Elk1 phosphorylation by ERK1b are caused by abrogation of the regulatory C-terminal sequence of ERKs. *J. Biol. Chem.* *276*, 35280–35289.